SpaceOps Conferences
5-9 May 2014, Pasadena, CA
SpaceOps 2014 Conference

10.2514/6.2014-1919

Lunar Optical Communications Link (LOCL) Demonstration between NASA's LADEE Spacecraft and ESA's Optical Ground Station

Igor Zayer, Robert Daddato, Marco Lanucara, Klaus-Jürgen Schulz
European Space Agency, ESA-ESOC, Robert-Bosch-Str.5, Darmstadt, D-64293, Germany

Zoran Sodnik, Hans Smit, Marc Sans
European Space Agency, ESA-ESTEC, Keplerlaan 1, Noordwijk, NL-2201AZ, The Netherlands

Johan Rothman
CEA-Leti/LIR, 17 rue des Martyrs, Grenoble Cedex 9, F-38054, France

and

Dirk Giggenbach, Peter Becker, Ramon Mata-Calvo, Christian Fuchs
German Aerospace Center, DLR-IKN, Wessling, D-82234, Germany

NASA's Lunar Atmosphere and Dust Environment Explorer (LADEE) spacecraft has embarked the Massachusetts Institute of Technology (MIT) - Lincoln Laboratory's (LL) Lunar Lasercom Space Terminal (LLST) as a secondary payload and part of the Lunar Laser Communications Demonstration (LLCD) experiment. The LLST was operated on four out of every seven days for one month during the commissioning phase of the LADEE spacecraft in lunar orbit, and then again for a shorter period of time, after the end of the primary scientific mission. ESA's Optical Ground Station (OGS) on the Canary island of Tenerife was one of two secondary participating ground stations – together with JPLs Table Mountain facility – involved in the experiment. We present, from ESA's perspective, the Lunar Optical Communications Link (LOCL) project including first results and lessons learned of the short-duration experiment using the OGS. The success of LOCL is of strategic importance for ESA for the development of future optical communications over "deep-space" distances.

I. Introduction

In September 2013 NASA launched the Lunar Atmospheric and Dust Environmental Explorer (LADEE) spacecraft, whose main mission is to study the pristine state of the lunar atmospheric and dust environment using several scientific payloads[1]. It also carries the Lunar Laser Communication Demonstration (LLCD) payload for high speed optical communications from lunar distance (up to 622 Mbps downlink and up to 20 Mbps uplink)[2]. The LLCD project has been developed by NASA's Goddard Space Flight Center and MIT Lincoln Laboratory and consists of the lunar laser space terminal (LLST) and the lunar laser ground terminal (LLGT), a transportable optical ground station located on the White Sands Complex (WSC), New Mexico[3]. The Jet Propulsion Laboratory (JPL) and the European Space Agency (ESA) have been given the opportunity to participate with their own specific ground facilities, namely the JPL Optical Communication Test Laboratory (OCTL) on Table Mountain, California, and the ESA Optical Ground Station (OGS) in Tenerife. The Lunar Laser Space Terminal (LLST; Fig. 1) was repeatedly operated for four days, followed by three days of non-operation during the

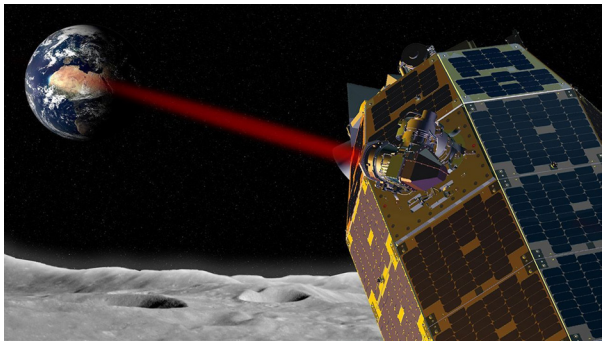

Figure 1. LLST aboard the LADEE spacecraft transmitting to a ground station (artist's impression)

commissioning and testing phase of LADEE. During this period, the satellite was in a ~2 hour lunar orbit at an altitude of about 200 km. The LLST operations were limited in duration to 15-20 minutes per orbital pass driven by on-board power resources and thermal constraints. Table 1 lists the main characteristics of the experiment.

Table 1. Main LOCL link parameters

Parameter	Description	Value	Unit
Range	Lunar distance variation	362570 - 405410	km
Wavelength	Beacon, Uplink, and Downlink wavelengths separated each by ~9 nm	within 1550 - 1568	nm
Modulation Format	Downlink:	16-PPM	
	Uplink:	4-PPM	
	FEC encoding:	SCPPM	
Data Rate	Downlink (Modes 5 - 1):	38.55 – 616.84	Mbps
	Uplink:	9.64 - 19.28	Mbps
LLST Transmit power	Optical transmit power	0.5 (nominal)	W
Downlink Irradiance	At the top of the atmosphere	0.17 - 1.7	nW/m^2
Uplink Irradiance required	At LADEE spacecraft	36 - 63	nW/m^2

II. ESA's Optical Ground Station (OGS) for LOCL

ESA maintains an optical ground station (OGS) at the Teide observatory on the Canary island of Tenerife[6] (cf. Fig. 2). ESA's OGS has served throughout many optical communication experiments involving space-ground links from the early days of the ARTEMIS spacecraft as well as inter-island experiments between the OGS and the neighboring island of La Palma through approximately 150km of atmosphere[4,5].

Figure 2. The Teide observatory (left) and ESA's OGS (right). With Teide, Spain's highest mountain, in the background and the Island of La Palma in the distance to the right in the left pane.

To enable ESA to participate in the demonstration using LADEE, the following had to be accomplished to realize the LOCL project in a very short time frame:

- Establish a legal framework within which the cooperation with NASA and all partners could take place
- Provide a receiver signal chain capable of communicating with LLST
- Provide a laser transmitter system
    1. as a beacon for acquisition and tracking
    2. for data up-link capable of communicating with LLST
- Implement design changes at the telescope to accommodate the various sub-systems
- Implement corresponding modifications to the OGS control system, including ground communications between the OGS and Lunar Lasercom Operations Center (LLOC) located at MIT-LL.

DLR-IKN participated in the experiment through a cooperation agreement with ESA by providing atmospheric turbulence measurements, using a power sensor at a coaligned 20-cm-telescope.

The overall architecture of the OGS setup for LOCL is depicted in Fig. 3.

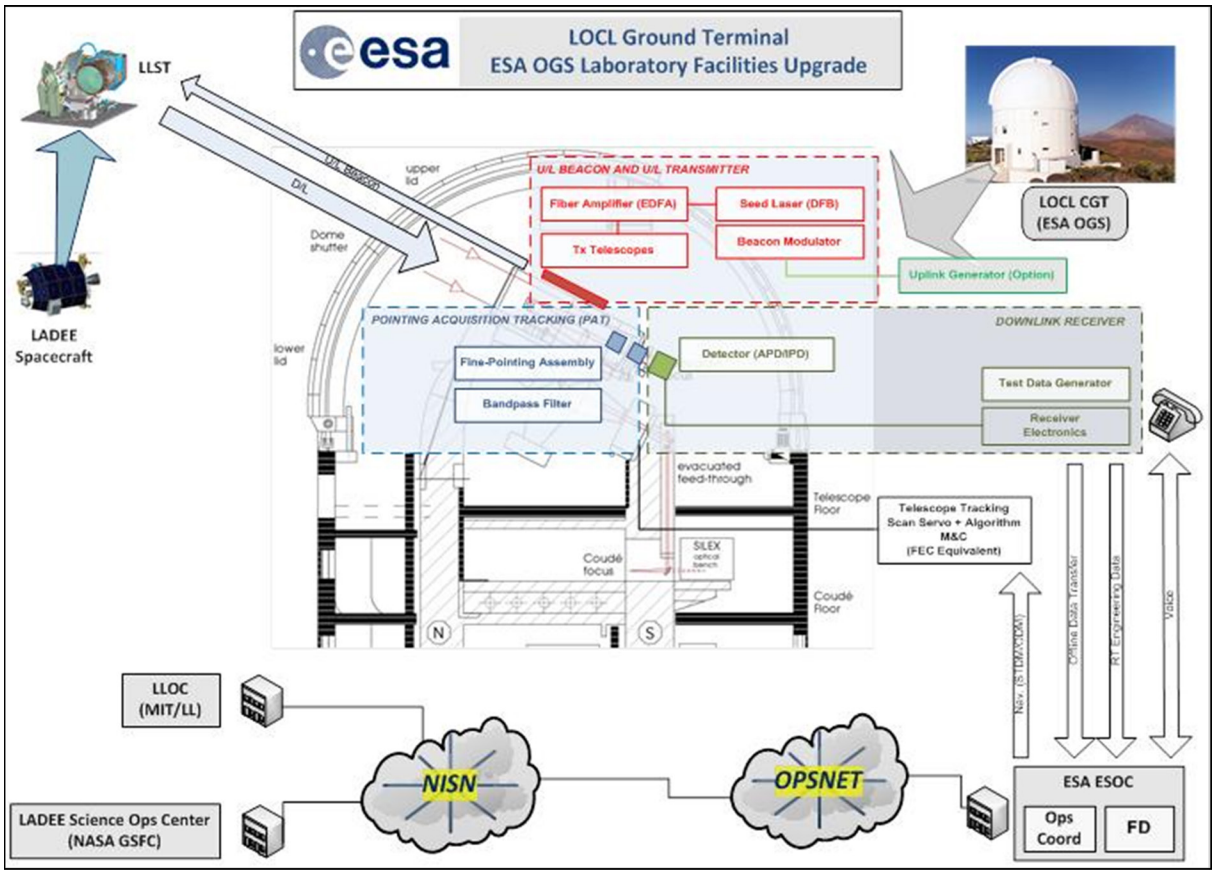

Figure 3. Different functional elements of ESA's LOCL experiment

A. The OGS Telescope

The considerations that governed the design adaptations in the OGS were the following[8]:

- The ratio between the required transmit power and the power received (130 dB) would require a bi-static design to avoid stray light from the transmitter to flood the highly sensitive signal chain.
- The telescope tube stiffness would provide stability to within a few µrad during the ~30 minute communication link with respect to deformations from gravity, such that the transmitter and the receiver would remain in alignment without active compensation.
- The stiffness of all three externally mounted transmitters would provide stability to within a few µrad with respect to beam deviations by gravity and would remain in alignment without active compensation.
- The use of wavelengths around 1550 nm combined with excellent seeing conditions at the OGS result in atmospheric image motion of a few µrad would only require a low bandwidth telescope tracking control. In addition, the link budget would not allow splitting sufficient light away from the communications receive path for high-bandwidth closed-loop tracking using the ATC.

The above considerations led to the installation of the focal plane instrumentation at the telescope's primary Cassegrain focus (Fig. 5) rather than on the optical bench in the Coudé room. The former consisted of both an InGaAs 2-D acquisition and tracking camera (ATC) and a fiber-coupler with a 200µm core graded-index multi-mode fiber (MMF). The fiber diameter corresponds to ~3 arc seconds field-of-view allowing to entirely couple the scintillating point spread function (PSF) under the expected seeing conditions at the observatory without real-time tip-tilt correction. A polarizing beam-splitter in combination with a quarter wave plate (QWP) allowed controlling the distribution of light between the ATC and MMF so as to maximize the communication link budget, while keeping the minimum necessary light on the ATC after having initially acquired the satellite. A filter wheel allowed the selection between five filter positions: open, block, 1064 nm, wide (1550.12 ± 2.5 nm), and narrow (1550.12 ± 1.2 nm). LOCL operations were conducted using the 'wide' filter position, whereas alignment and calibration activities using a retro-reflector (cf. below) were performed in the 'open' position.

Furthermore, an InGaAs photoreceiver was mounted at the focus of a coaligned 20–cm-telescope, which is attached to the main telescope. With its one meter diameter, the main telescope strongly averages the power scintillation, because the atmospheric coherence length is much shorter than the telescope diameter. The purpose of this photodetector was to monitor the received power with a smaller averaging aperture. In order to limit the amount of background light collected by the receiver, a narrow optical filter (1550.9± 1.2 nm) was set before the

detector. The receiver was characterized before the measurement campaign, by measuring the power sensitivity under laboratory conditions with a CW laser signal[11]. The power sensitivity was measured around 1 pW and saturation was reached at 250 pW for a transimpedance gain of $2x10^{10}$.

In Fig. 4, the 20-cm-telescope and the InGaAs detector with the filter are shown. The receiver was fixed to the telescope with a dovetail adapter plate and was adjustable in three axes by micrometer screws.

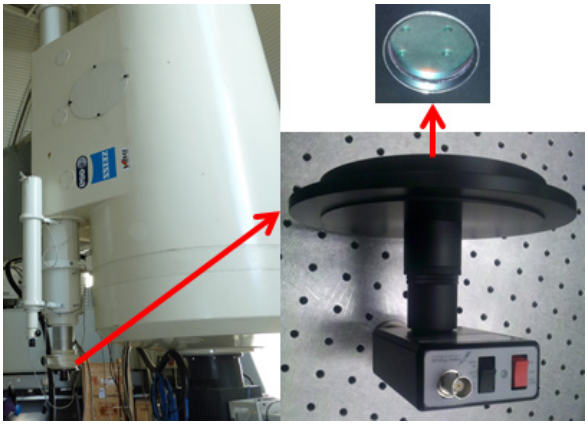

Figure 4: Power Receiver at the 20cm telescope

B. Transmitter Design

In order to mitigate atmospheric effects on the uplink (affecting the link more severely than on the downlink due to the so-called shower curtain effect); three separate laser transmitters were mounted on the perimeter of

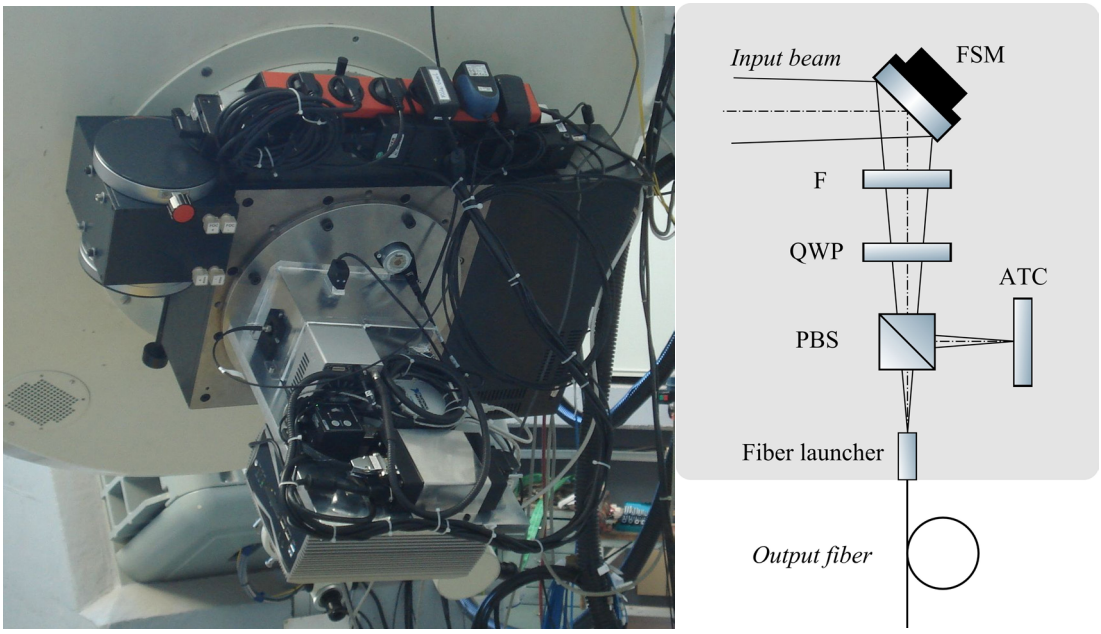

Figure 5. Receiver focal plane in the primary focus of the telescope (FSM: fine steering mirror, F: selectable filter, QWP: quarterwave plate, PBS: polarizing beam splitter, ATC: acquisition and tracking camera)

the telescope aperture (cf. Fig. 6). The three beams overlap incoherently at the LLST, thereby minimizing the occurrence of signal outages in the far field (e.g. dark areas in the speckle pattern). Mutual incoherence was established by de-tuning the individual laser sources (both for the acquisition and the communication wavelengths) while still remaining within LLST's respective band-pass filters. Furthermore, using multiple transmitters permitted to increase the optical transmit power, since a single amplifier found on the market provided 40W maximum output power.

The seed laser sources and the modulators were installed in a rack in the Coudé room feeding fiber amplifiers mounted on the telescope tube itself, thereby keeping the output optical fibers between the amplifiers and beam expanders sufficiently short to avoid any non-linear effects. Two sets of 3 lasers (one set each for the acquisition and communication wavelengths, respectively) were installed in so-called ModBoxes from Photline. Whereas the communication signal was modulated as a 4-ppm pulse-train via external modulators within the ModBox, the acquisition beam called for a 1 kHz square-wave modulation which was achieved by modulating

the pump diodes of the amplifiers themselves. Non-linear and other effects in the amplifiers were driving additional implementation solutions:

1. in order to avoid stimulated Brillouin scattering (SBS) induced by the very narrow acquisition laser lines, the three individual acquisition laser sources were combined such that each amplifier was fed by two sources in cyclical order rather than having a one-to-one correspondence (not evident from the simplified scheme shown in Fig. 6). Thus, amplifier nr.1 was fed by acquisition laser sources 1 + 2, nr.2 by 2 + 3, etc., such that the two slightly de-tuned wavelengths suppressed SBS. This combination was not necessary for the communication lasers since the > 10 Mbps 4-ppm pulses broadened the spectral line width sufficiently.
2. the relatively slow 1 kHz square-wave modulation of the acquisition lasers would have destroyed the amplifiers due to a burst-wise depletion of energy accrued within the amplifier during the relatively long dark period between consecutive square pulses. Therefore, only the 3rd (last) stage of the amplifier was modulated, leading to a reduced overall output power for the acquisition beacon but sufficient to ascertain LLST's tracking. Alternatively, a "filler" laser modulated at 1 kHz in anti-phase to the acquisition lasers (but sufficiently offset wavelength in order not to be recognized by LLST), as implemented by MIT-LL, could have been used.

The communication signal was generated by an uplink signal generator system (ULD) built by Axcon, driving the external modulators in the communications ModBox. In addition to generating the 4-ppm modulation compatible with LLST using selectable data types (idle frames, pseudo-random bit sequences (PRBS-31), user-provided data), data rates (10 or 20 Mbps) and interleaver modes, the system performed correlation between sent and received frame alignment sequences (FAS; as part of the communication frame structure). The later allowed for a relative time-of-flight ranging capability.

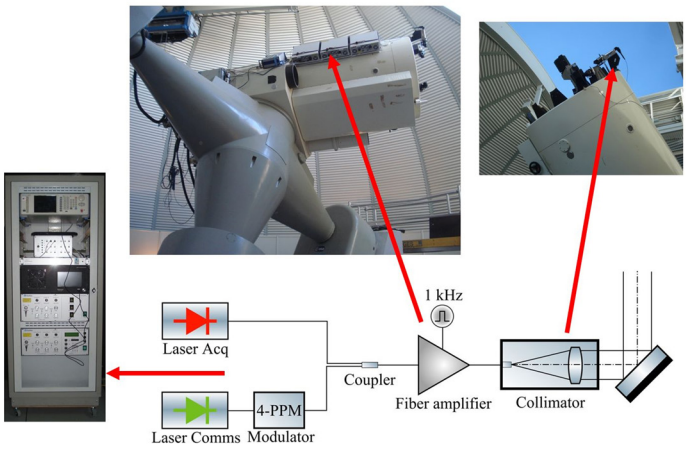

Figure 6. Laser Transmitter sub-system (three separate beams are implemented).

In order to ascertain a well-defined pulse train arriving at LLST, the temporal co-alignment of pulses between the three transmitters had to be adjusted to within less than 0.1 ns. This was only possible after the installation of the entire system at the OGS by measurements using fast photodiodes directly at the transmit apertures and a high-speed oscilloscope. Significant path differences (>5 meters in coax) were observed (due to differences in fiber lengths mostly within the amplifiers) and compensated by adjusting the lengths of co-axial cables between the drivers output of the ULD and the ModBox modulators input.

C. Receiver Chain

The receiver chain was developed by RUAG Space in Zurich, Switzerland under an ESA contract[10]. It comprises fiber-coupled detectors, raw pulse synchronization, real-time data buffer, off-line de-interleaver and decoder together with a downlink transmitter simulator and associated fiber laser (cf. Fig. 7). The latter enables testing of the entire receive path with properly calibrated optical power settings through an optical attenuator between the fiber laser and fiber-coupled detector(s). This test setup has been validated through comparison with the MIT-LL Test Kit (cf. Section III).

1. Detectors

Whereas the LLCD experiment had been designed with super-conducting nano-wire sensors as the baselined efficient photon-counting detectors, this technology was not available for the LOCL project. Intensified avalanche photo-diodes (IPDs) had been identified as the most promising solution at project start. During a critical decision point in the project it became evident that IPDs could not be produced and delivered for LOCL. Suitable alternatives were intensely sought and two potentially promising solutions were pursued in parallel – ultimately with success (cf. Fig. 8):

a) Photo-multiplier tubes (PMT) from Hamamatsu
b) HgCdTe (MCT) avalanche photodiode (APD) in linear mode from CEA-Leti/LIR

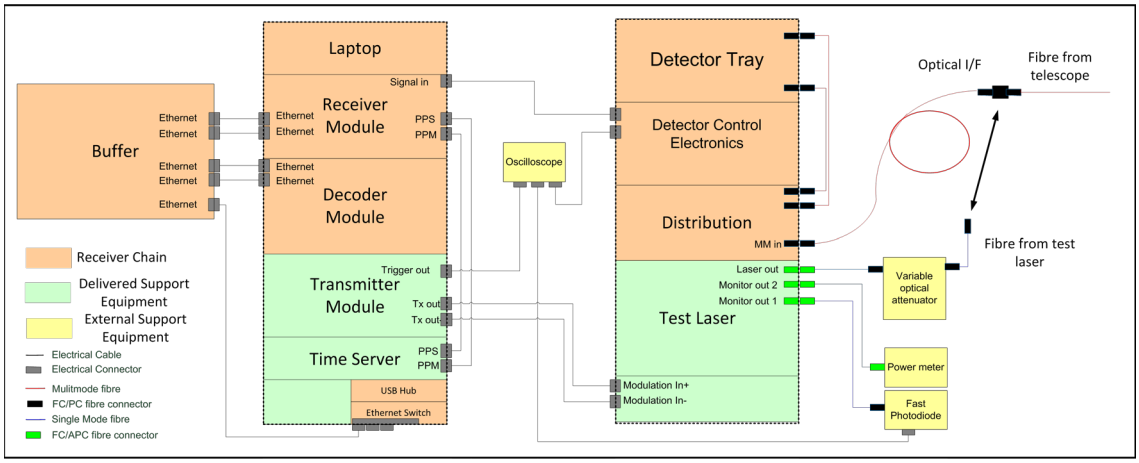

Figure 7. Block diagram of RUAG receiver chain.

The commercially available PMTs were baselined after initial evaluation by RUAG. Driven by the fact that their primary application is single-photon counting, both their lifetime and behaviour (after-pulsing) is severely impacted by over-exposure. To overcome this limited dynamic range, the light would be split onto several individual PMTs in parallel to decrease the overexposure probability and to increase the detection probability – the budget allowed for two devices.

Figure 8. The LOCL receiver chain (left) with the Hamamatsu PMT's mounted in the right rack, and the Leti MCT APD with fiber-coupler lens (right)

The MCT APD was pioneered at CEA-Leti/LIR by Dr. Johan Rothman and was pursued at first as a back-up detector. It became available just in time for integration into the LOCL experiment in October 2013. Due to weather, however, this first prototype did not see operation in that first phase. The opportunity of a second, short, demonstration phase in early April 2014 allowed a newer generation APD prototype to be assembled, tested and installed at the OGS where it has been operated very successfully, capable of supporting the LLST downlink mode with 154.20 Mbps (exceeding the capability of the receiver system, however).

The raw, pre-amplified, electrical detector signal was fed both to the receiver chain and to the ULD system (both implementing the same type ADC board) via a splitter in order to perform time-of-flight (relative) ranging through time correlation of transmitted and received frames performed by the ULD system. Changing between the two detector systems entailed reconnecting the MMF fiber from the telescope and the electrical signal cables (both the receiver board and the ULD) to either of the chosen detectors which could be achieved within one minute.

2. Receiver module

An ADC samples the analog pulse-train from the detector and the digital data stream is then synchronized by recovering the clock in order to phase lock onto the signal. The frame alignment sequence (FAS) is used to detect subsequent downlink frames. In addition, first-order performance is established using the FAS including the symbol error rate and other engineering parameters. The output of this module consists of slot values of the detected frames which are transferred to the buffer via a high-speed interface.

3. Buffer server

Since most of the receiver chain was not designed to support real-time processing, a high capacity data buffer (RAID storage in server configuration) records the raw PPM slot values during communications as well

as above-mentioned engineering parameters. Channel de-interleaving and SCPPM decoding is performed by off-line post-processing of data stored in the buffer (which then serves to store the processed telemetry)

4. De-interleaver

To mitigate atmospheric effects on the link, LLST supports 6 Forney convolutional interleaver modes on the down-link with different storage lengths which result in outage compensation capabilities of durations between 0 and ~1.5 s. The channel de-interleaver has been implemented in software running on the receiver control computer, taking approximately 20 min of computing time for a few seconds of data. A compiled version running on the Buffer server allowed de-interleaving 1min worth of data in 45 s.

5. Decoder module

Finally, an iterative SCPPM turbo decoder comprising four inner and eight outer decoders was implemented in an FPGA in the decoder module. It has been developed in collaboration with the Integrated Systems Laboratory at the ETH Zürich[7]. The decoder is clocked with 100 MHz achieving the required throughput of 39 Mbps with 20 iterations; it reads de-interleaved data from the buffer and writes back de-coded data

D. Telescope Control System

The adaptations to the OGS control software was one of the most complex to be implemented at the OGS as evidenced by its architecture depicted in Fig. 10.

Various computers control specific sub-systems (AXCON: ULD system; RUAG: receiver chain and buffer server; RTCC: ground communications link and ModBox; FPPC: telescope focal plane incl. ATC and laser amplifiers; TTC: telescope tracking computer commanding the TCC: telescope control computer) running corresponding applications that, in turn, are commanded from the main 'ogs_gui' control software application as the operational console during the communications link. Furthermore, a computer (labeled ESOC) located in ESA's ESTRACK control center provides data packetization and relay between ESA's OPSNET network and NASA's NISN.

III. Inter-Operability Testing

Figure 9. ESA-NASA inter-operability testing at RUAG Space

While all LOCL sub-systems for the OGS (including the new detector, buffer and decoder, the beacon and uplink transmitters, the uplink modulator and ranging correlator) have been functionally tested as far as possible in their stand-alone configuration, the ultimate verification of compatibility with LLST could only be established by interoperability tests carried out with a Test Kit provided by MIT-LL, simulating the bidirectional acquisition and communication signals of LLST. The transportable, rack-mounted, MIT-LL Test Kit had already been used in the actual validation and testing of both Lincoln-built Space and Ground terminals. The testing with the Test Kit was of utmost importance for the success of the demonstration.

During the week of 19 June 2013 (2.5 Months before launch!), ESA together with its European industrial partners RUAG (CH), Axcon (DK), and CEA-Leti (F) assembled the different sub-systems at RUAG's premises while NASA with MIT-LL experts operated the Test Kit (cf. Fig. 9).

This inter-agency optical compatibility test was the first of its kind, and it has proven crucial in identifying and correcting discrepancies in sub-systems that had been built to specifications purely according to a paper Interface Control Document (ICD). The week-long campaign ultimately established compatibility for the uplink, downlink and the ranging as well as confirmed expectation values for performance as a function of optical power levels. Very importantly, the testing validated RUAG's transmitter simulator system.

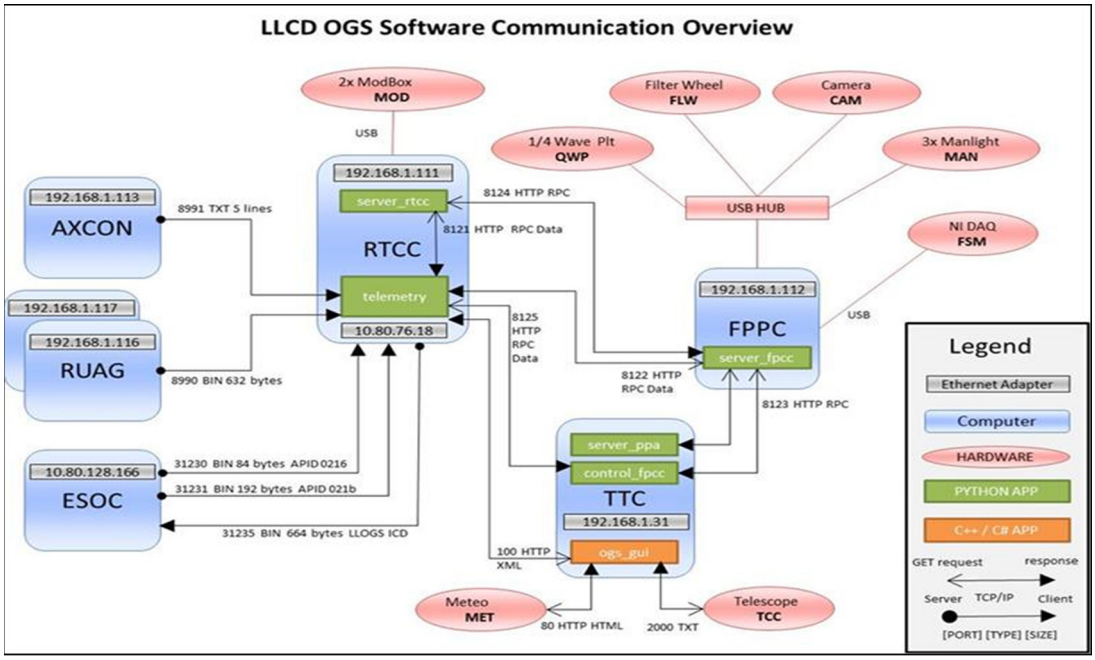

Figure 10. Block diagram of LOCL control system software.

IV. Operations

1. Concept of Operations

The schedule of supported passes was established by LLOC on a weekly basis within each campaign, by defining a primary and a back-up terminal for each supported slot. The preparation for each pass began, at the OGS, around two hours prior to the expected earliest begin of track (BOT), and included a voice check with LLOC, a briefing on the planned activities during the pass (e.g. switching of telemetry modes), the execution of the transmitter co-alignment procedure, and a verification of the weather conditions around 30 minutes prior to BOT, leading to the final go-ahead for the pass. Shortly before BOT, LLOC was reporting about the expected detailed time of switch-on of the on-board power.

The activities during each pass started with the uplink acquisition on the acquisition wavelength, immediately followed by the downlink acquisition, and by the required switching of telemetry modes. It was intended to switch to the uplink communications wavelength during most of the passes, which proved to be very difficult, as detailed in Table 2, which shows a summary of the activities performed for passes between 26 October and 2 November 2013. The selected on-board and OGS parameters were visible at OGS and LLOC respectively through the established ground-to-ground interfaces, thus allowing a quasi-real time coordination of the activities on each side. Each slot lasted around 20 minutes, the on-board transmit duration being limited by power and thermal constraints. One pass not requiring on board transmission (#5 on 29 October, devoted to monitor the received uplink power during OGS spiraling, to individually characterize each transmitter's misalignment) lasted almost one hour.

Table 2. Summary of main activities during passes between 26 October and 2 November 2013.

Date	Pass Id	OGS role	Pred. BOT [UTC]	Actual BOT [UTC]	EOT [UTC]	Approximate duration [UTC]	Main activities
26/10/2013	#1	Prime	06:07:00	06:36:17	not recorded	not recorded	First downlink acquisition, first attempts to go to uplink communications after uplink acquisition, no telemetry recorded
26/10/2013	#3	Prime	10:07:00	10:12:00	not recorded	not recorded	Attempts to optimise received uplink power by scanning, only dew seconds of telemetry recorded
27/10/2013	#1	Prime	03:37:00	03:43:00	04:09:32	00:26:32	Telemetry reception, received uplink power on-board monitored, between -80 and -77dBm
27/10/2013	#2	Prime	06:13:00	06:15:37	06:37:50	00:22:13	Telemetry reception, with various modes supported. Spiralling attempted to optimise uplink pointing.
27/10/2013	#4	Back-up	10:10:00	n.a.	n.a.	n.a.	Pass not followed (OGS was back-up)
28/10/2013	#1	Prime	03:39:00	03:58:00	04:10:00	00:12:00	Pass planned on optimising received uplink power by spiralling, while keeping LLST tracking mode disabled, however cancelled few minutes after BOT due to weather.

Date	Pass Id	OGS role	Pred. BOT [UTC]	Actual BOT [UTC]	EOT [UTC]	Approximate duration [UTC]	Main activities
28/10/2013	#2	Prime	06:17:00	n.a.	n.a.		Pass cancelled due to weather
28/10/2013	#4	Back-up	10:12:00	10:18:00	11:05:00	00:47:00	First part of the pass focused on telemetry recording, second part attempting to go to uplink communications. Investigation on individual transmitters pointing by switching one transmitter at the time
29/10/2013	#1	Prime	03:41:30	03:59:55	04:22:05	00:22:10	Telemetry recording, with monitoring of uplink power and attempt to go to uplink communications.
29/10/2013	#2	Prime	06:19:00	06:19:28	06:42:00	00:22:32	Same as pass#1 during the same day.
29/10/2013	#3	Prime	08:16:00	08:17:00	08:39:43	00:22:43	Same as pass#1 during the same day.
29/10/2013	#5	Back-up	12:52:30	13:03:06	13:26:19	00:23:13	LLOC proposes a systematic spiralling to investigate the misalignment. The exercise reveals around 10 arc seconds offset on one transmitter (TX3). Same exercise for the other two transmitters aborted due to weather.
02/11/2013	#2	Prime	08:34:00	08:43:00	09:05:00	00:22:00	Pass focused on telemetry recording, with monitoring of uplink power and attempt to go to uplink communications
02/11/2013	#3	Prime	10:35:00	10:44:00	11:07:00	00:23:00	Same as pass#2 during the same day, including an attempt to perform time-of-flight (TOF) measurements. Uplink Rx power always below the threshold to enable fine tracking on the communications wavelength.

2. Transmitter co-alignment

By applying offsets to the fine steering mirror (FSM) and thereby offsetting the boresight of the receiver it was possible to change the pointing of the telescope tube (while keeping the received beam centered on the receiver fibre), it was only possible to adjust the pointing of the telescope itself (thus all three transmitters - mounted on the rim of the telescope's aperture - jointly). Therefore it was necessary to co-align all three transmit beams which, during the main campaign in 2013, consisted in adjusting the micrometer screws of the folding mirrors in each of the three beam-expanders (Fig. 11) prior to each pass. This was done while holding a retro-reflector cube in front of each transmit aperture in sequence while monitoring the position of the reflected spot on the ATC. Since creep in the adjustment mechanisms and distortions of the telescope tube caused the pointing of the beams to drift, said adjustment was carried out at a telescope position corresponding to the middle of the pass. Despite this attempt to minimize the pointing errors it proved impossible to achieve the expected irradiance at the LLST. Furthermore, the alignment procedure was not feasible for some of the passes, because it was physically impossible to reach the aperture beyond certain elevation limits.

Figure 11. Adjusting the coarse micrometers by one of the authors (left) while holding the retro-reflector (right) in front of each transmitter.

In anticipation of a second LOCL campaign in 2014, a closed-loop pointing control system using an internal guide laser had been designed and partly implemented. Unfortunately, a critical dichroic beam-splitter was not delivered in time, preventing full deployment of the former. The alignment improvement for the second campaign consisted in the ability to individually control each of the three transmitter folding mirrors, albeit in open-loop.

The co-alignment procedure during 2014 thus consisted in a calibration run, during which the retro-reflector was mounted in front of one transmit aperture and the telescope was tracking the anticipated LADEE pass (with a 20 x faster speed). The motion of the back-reflected spot on the ATC was recorded and corresponding corrections applied to the piëzo-driven folding mirror. The telescope was again commanded to simulate tracking

of the pass to verify stable centering of the spot. The retro-reflector was then replaced by a counter-weight simulating its mass on the transmitter mount, and the entire procedure was repeated for each of the three transmitters. Repeated calibration runs provided initial confidence that the repeatability of the setup to within 1-2 arc seconds would lead to a sufficiently stable co-pointing of the three beams during the pass. Unfortunately, repositioning the telescope away from the tracking arc of the anticipated pass (e.g. to dis-/mount the retro-reflector) proved to invalidate the corrections due to the poor mechanical rigidity of the beam expanders within the required accuracies. Worse yet, sun illumination / heating of the telescope tube after opening the dome for the actual pass led to misalignment.

3. Satellite Acquisition and Tracking

During most link sessions, the accuracy of the satellite tracking data as well as the telescope pointing was excellent and the laser beam from the LADEE spacecraft would be acquired immediately after switch on of the LLST. The OGS would transmit a 1 kHz modulated beam at full power (60 Watts average) from its three transmitters, however, due to alignment problems, usually only one transmitter contributed to the uplink irradiance.

Tracking started immediately after acquisition, but first the optimum uplink pointing direction had to be determined. This was done by scanning the uplink beam until the irradiance on the satellite was maximized (monitored by online telemetry and exchanged via a ground based network). As it turned out the optimum Tx pointing direction did not coincide with the receive beam from LLST being centred on the ATC and receive fiber and the misalignment was compensated by applying an offset to the fine steering mirror (FSM). Once this alignment was achieved the received beam was controlled to stay in the centre of the ATC by applying offsets to the telescope tracking, either automatically (every 6 seconds) or manually. This led to beam wander beyond the receive fiber area and caused additional intensity fluctuations, which should be avoided by implementing an automatic tracking system at higher speed.

V. First Results

Over the course of the communications demonstration, the ESA-OGS succeeded in achieving the following objectives:

- Routine, sustained telemetry downlinks.
- Synchronization of the LLST clock to the ESA-OGS clock, demonstrating two-way time of flight measurement capability.
- One short duration optical data uplink.

1. Telemetry downlink

During the two optical communication campaigns in 2013 and 2014, a total of more than 5,800 seconds of downlink time was accumulated at the ESA-OGS during communication passes. The successful data downlinks were performed in downlink mode 5 at a data rate of 38.55 Mbit/s, during which a total of over 95 Gbit, corresponding to 2,500 s, of data in error-free frames was received.

The average signal power received at the communications detector was on the order of (170 ± 70) pW, with signal fades of up to 10 dB or more occurring randomly (depending on atmospheric conditions). The timescale of the signal power variations was observed to be around 50 ms according to the first change of slope of the autocorrelation function. (Figs. 12, 13).

With the Hamamatsu PMT, the receiver was shown to have a signal power threshold of about P_{thr} = 50 pW, above which the receiver was error-free (Fig. 14).

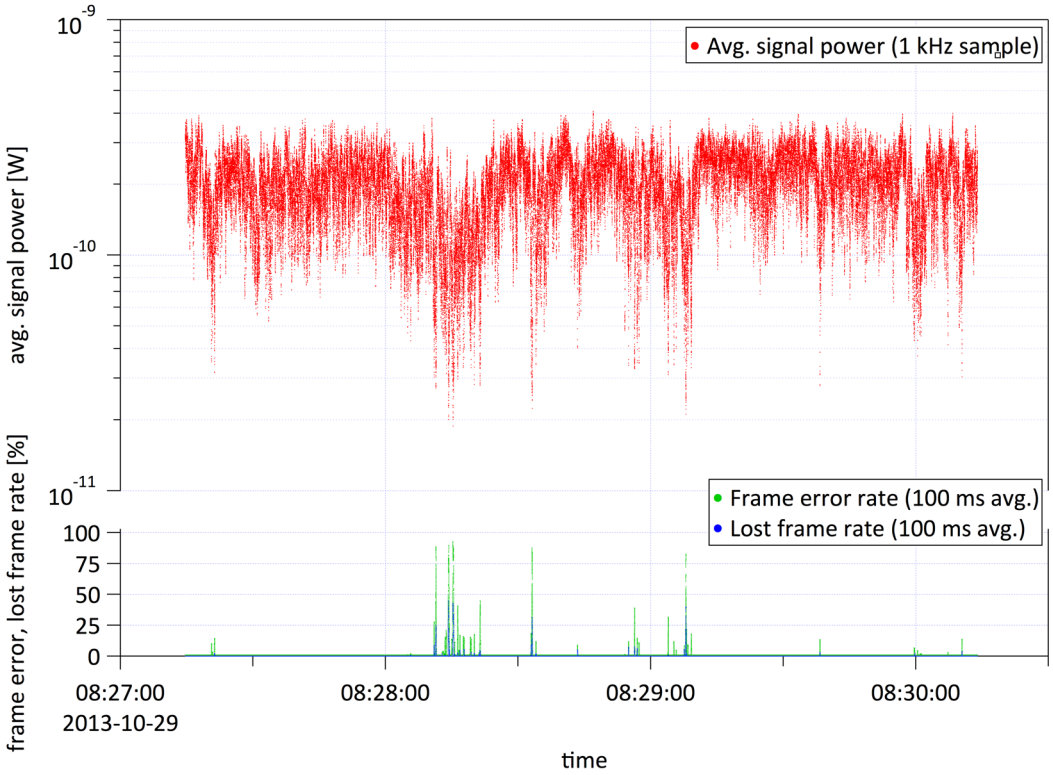

Figure 12. Signal power variation at the receiver and lost frame/frame error rates during successful downlink reception. Unexpected low average signal power, high signal fluctuations and deep fades occur, during which the frame error rate becomes significant.

With the average power therefore at a level of (3.4 ± 1.4) × P_{thr}, downlink data received in mode 5a exhibited an average frame error rate of 4%. The analysis of data recorded in other interleaver modes is still ongoing.

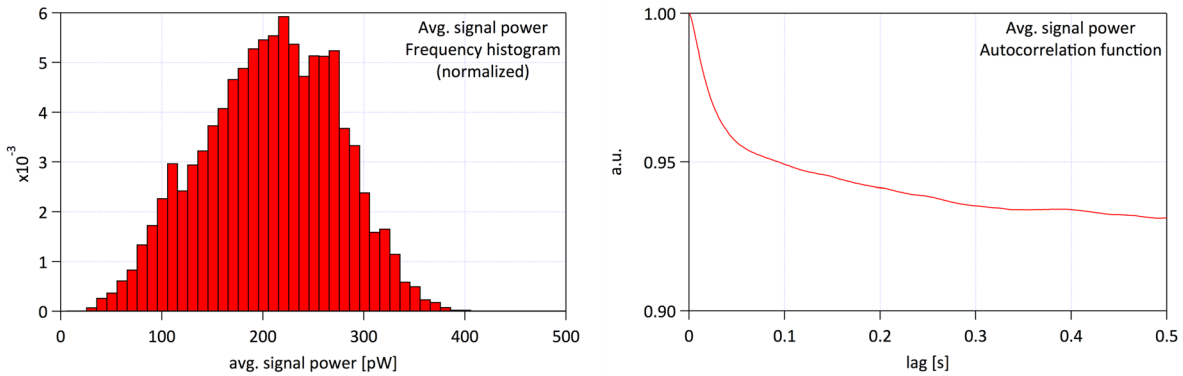

Figure 13. Typical frequency histogram and autocorrelation function of the average signal power during a successful data downlink.

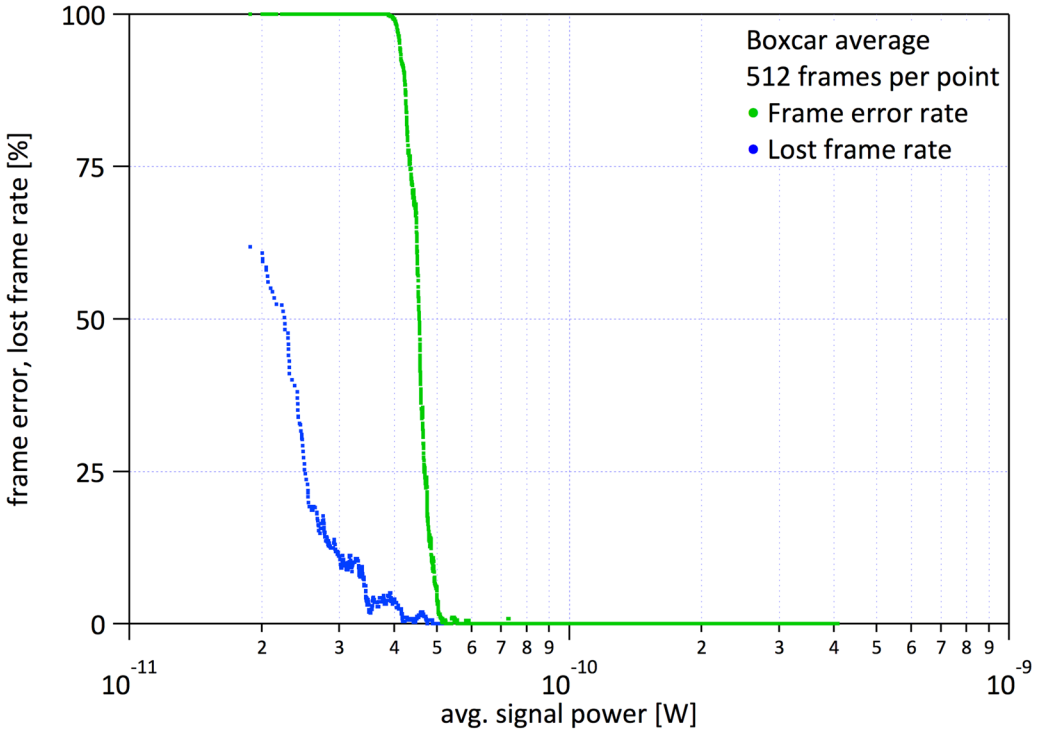

Figure 14. Lost-frame rate and frame-error rate (both averaged over 100 ms) as a function of average signal power at the Hamamatsu PMT detector. There is a threshold of about 50 pW, above which reception is error-free.

2. Received power at the 20-cm-telescope

Approximately 1 hour of valid received power measurements were recorded. Sunlight scattered from the lunar surface was responsible for an offset of up to 100 pW. The actual average received signal power was in the range between 9 and 25 pW at 0.5 W transmit power (see Fig. 15). During acquisition at the beginning of the measurement, the signal was attenuated by clouds. For a short time after around 00:55 on 19. November 2013, the transmit power was increased to 1 W before switching off the transmission. The measurement was continued after that to get information about the background light level. The large detector area and therefore large field of view leads to averaging of background light, thereby reducing scintillation in this part.

In Fig. 16 the normalized probability density functions for different elevation angles are displayed. For low elevation angles, the maximum of the normalized PDF shifts to lower Rx-power, as expected. These plots are sorted in order of measurement date in the following Table 3:

Table 3. Assignment of measurement date and time to elevation angle.

Date – Start time	Elevation [deg]
26/10/2013 – 06:30	77
26/10/2013 – 10:10	35
27/10/2013 – 03:35	42
27/10/2013 – 06:15	71
28/10/2013 – 03:45	33
19/11/2013 – 00:24	70

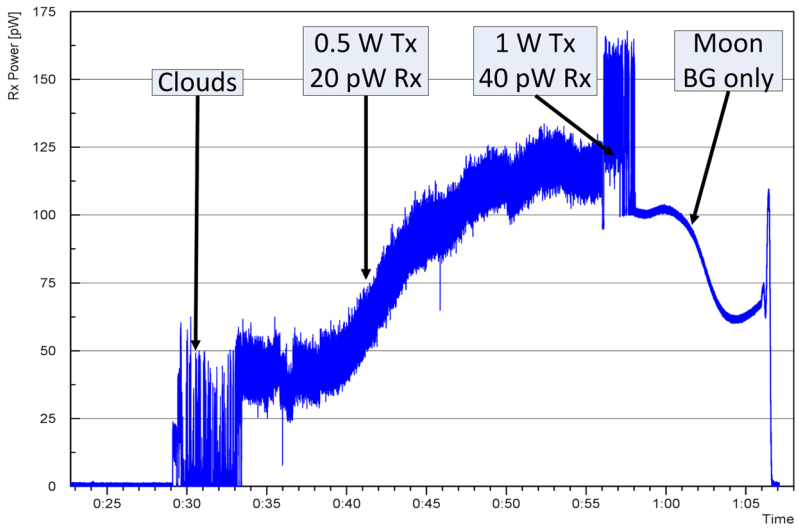

Figure 15 Example received power measurement from 19. November 2013. Background irradiance can reach up to ~100 pW while the average Rx-power is ~20 pW.

Since measurements were taken on different days, the turbulence conditions changed between measurements. This can be seen, for example, at 70° elevation, where a higher scintillation value than at 42° was obtained. In order to arrive at an estimate of the turbulence impact, the focus images of the ATC will be used to estimate the atmospheric coherence length. Focal speckle patterns from ATC are still being processed in order to estimate the Fried parameter. Values in the range between 8.1 cm and 14.1 cm have been calculated[12].

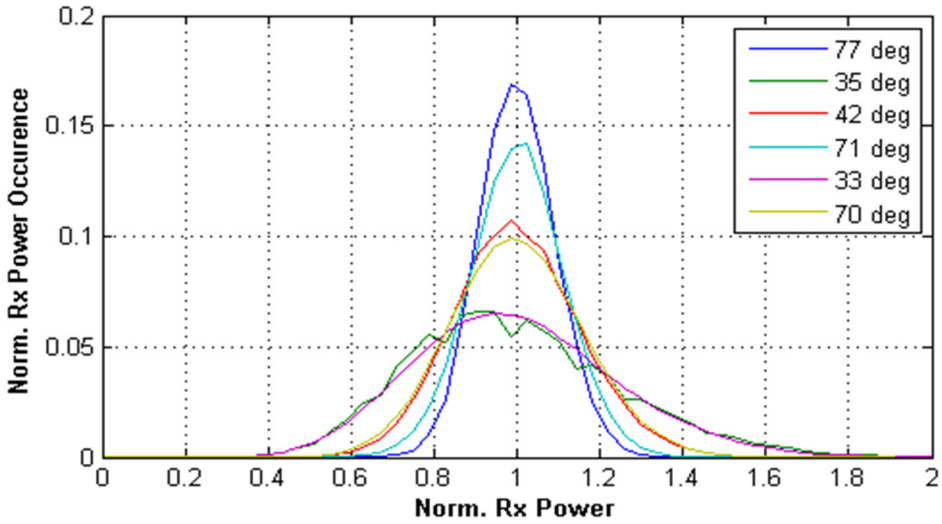

Figure 16 Received power PDF for different elevation angles at the 20-cm-telescope.

3. Clock synchronization and optical uplink

Due to the difficult alignment of the uplink transmitter telescopes, as reported in section IV. 1, the uplink signal strength recorded at the LLST was only sufficient to allow the onboard clock to track the uplink clock for about 69 seconds during one single pass. During the same pass, the LLST also reported error-free reception in uplink mode 2e for about 6 seconds.

The time at which the receiver clock on the LLST was tracking the uplink clock can be deduced from the low-rate RF telemetry returned to the ESA-OGS by the LLST (via the LLOC and ESOC). A valid nutator (fine tracking sensor) power indication and a flag indicating a lock of the receiver clock to the uplink signal (CLKREC_FSM_STATE = 13) occurred together during a pass on April 2, 2014 between 19:47:35.55 and 19:48:44.55 (UTC).

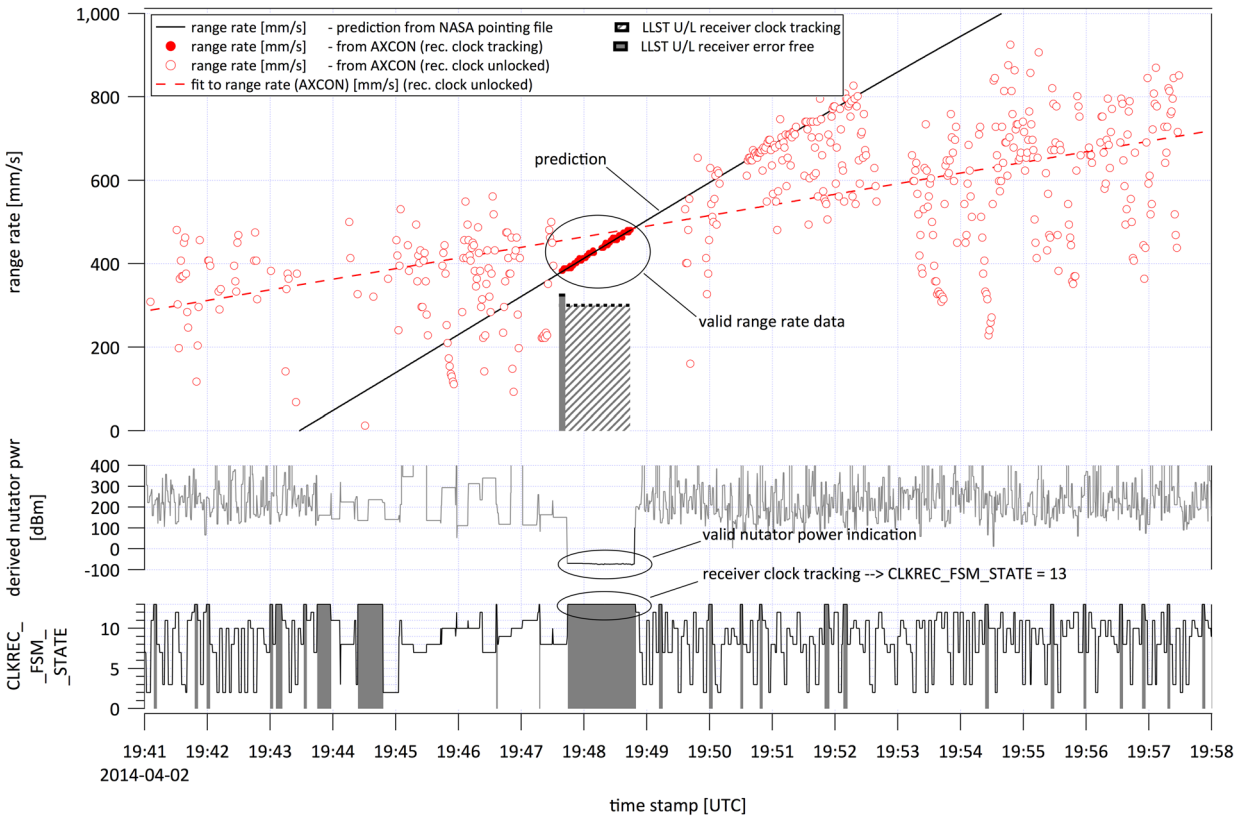

Figure 17. Timeline of communication pass that resulted in 69 seconds of valid two-way relative time of flight ranging measurements. Between approx. 19:47:35 and 19:48:44 the lower two plots show that the LLST clock reports it is tracking the uplink clock (CLKREC_FSM_STATE = 13) and simultaneously the power level received at the fine poining sensor returns a valid reading (derived nutator power = -72 dBm).

During this interval, the returned range rate values (upper plot, solid circles) are in good agreement with the prediction from the NASA pointing file (solid line). At times before and after the tracking lock, the returned range rate values (hollow circles) and their average slope (dashed line) strongly depart from the tracking predicition.

During this time interval, the correlation between sent and received frame alignment sequences performed by the ULD (s. section II.B) returned valid two-way relative time-of-flight ranging data (Fig. 17).

VI. Lessons Learned

Several conclusions can be drawn from the experiments that a future operational optical communications system will need to address:

- Inter-operability testing is essential to ascertain compatibility rather than relying on interface control documentation.
- Although aperture averaging by large diameter telescope apertures is known to effectively eliminate nulling of the received signal due to atmospheric scintillations, strong fluctuations in signal strength were observed during most of the passes. We attribute this to a combination of depointing due to atmospheric scintillation and depointing due to lack of closed loop tracking capability.
- Detectors: truly photon-counting detectors are optimized for very low signal levels, whereas the novel linear MCT APD provided very clean pulses in a slightly higher flux regime.
- To take full advantage of aperture averaging, the complete speckle pattern in the focal plane must be coupled into the fiber (or onto a detector) – either by increasing the fibre diameter, or by active tracking of the focal spot.
- Weather phenomena at observation sites can often be very localized and difficult to forecast.
- In an experiment environment such as LOCL, real-time interaction and intervention with the spacecraft operations center via a high-quality voice loop is invaluable.
- Ideally an automatic Tx/Rx alignment system, or a real-time monitoring of Tx/Rx alignment is required.
- In case of sub-optimal pointing files, or telescope pointing accuracy, a search pattern monitoring system is an important feature during initial satellite acquisition.

VII. Conclusions

The primary LOCL demonstration occurred during several dispersed slots in the period between October 26, 2013 and November 20. Approximately 50% of the links had to be cancelled due to bad weather, mainly in November (which is statistically the worst month for the Canary islands observatories).

The low uplink irradiance resulting from transmitter co-alignment problems in the OGS prevented a stable switch over from the acquisition to the communication wavelength, making it impossible to test data uplink and ranging during the first campaign in 2013. However, the LLST was acquired and tracked with successful demonstration of virtually error-free data reception (as expected, depending on the interleave modes) at data rates of 38.55 Mbps from the Moon.

A second, short LOCL campaign took place on April 1st – 3rd (with OGS being the primary/only ground station) with two scheduled passes on each of the three days. Again, weather only permitted to perform three out of five possible passes. Since a closed-loop beam pointing control system did not materialize in time, similar co-pointing problems prevailed, but time-of-flight ranging as well as error-free data uplink (at 10 Mbps) and downlink (at 71.10 Mbps with a novel detector) were successfully demonstrated.

The success of the LLCD experiment – and for ESA, LOCL – has contributed to an increased awareness of the capabilities of optical space links. LLCD has proven the benefits of cross-support in optical communications and thereby validated, among others, the work of the Optical Link Study Group (OLSG)[9], which resulted in the creation of an Optical Communication Working Group within CCSDS to elaborate standards that will facilitate future cross-support and inter-agency collaboration in optical space communications. LLCD / LOCL's successful demonstration was a contributing factor to the creation of the latter.

Acknowledgments

The authors are deeply indebted to John Rush and Donald Cornwell from NASA and to Don Boroson, Bryan Robinson, Steven Constantine and the LLCD team at MIT-LL as well as Farzana Khatri and the LLOC team for their support and the opportunity to participate in the experiment with LADEE. The authors would like to thank Joseph Kovalik from JPL, Fabio Gambarara, Martin Mosberger, Felix Arnold and Johannes Widmer from RUAG Space, Anders Enggaard and Torben Vendt Hansen from Axcon, Reinhard Czichy from Synopta, Sebastien Grot from 3SPhotonics/Manlight and Herve Gouraud from Photline for crucial support and helpful discussions, Kevin Kewin and Thomas Molitor (ESOC) for the implementation of the ground-to-ground interface and communications between OGS, ESOC and LLOC, and the Operations Team in ESOC, in particular Kenneth Scott and Martin Unal for the data transfer support during the campaigns.

References

[1]B. Hine, S. Spremo, M. Turner, R. Caffrey, "The Lunar Atmosphere and Dust Environment Explorer (LADEE) Mission," 20100021423, June 2010.

[2]B.S. Robinson, D.M. Boroson, D.A. Burianek, D.V. Murphy, "The Lunar Laser Communications Demonstration," *Proceedings of the International Conference on Space Optical Systems and Applications*, 2011, pp.54-57, 11-13 May 2011.

[3]M. E. Grein, et al., "Design of a Ground-Based Optical Receiver for the Lunar Laser Communications Demonstration," *Proceedings of the International Conference on Space Optical Systems and Applications*, 2011, pp.78-82, 11-13 May 2011.

[4]Romba J, Sodnik Z, Reyes M, Alonso A, Bird A, "ESA's Bidirectional Space-to-Ground Laser Communication Experiments". *SPIE Proceedings*, 2004 , Vol. 5550, pp. 287- 298.

[5]Reyes M, Alonso A, Chueca S, Fuensalida J, Sodnik Z, Cessa V, Bird A, "Ground to space optical communication characterization", *SPIE Proceedings*, 2005, Vol. 5892, pp. 589202-1– 589202-16.

[6]Sodnik Z, Furch B, Lutz H., "The ESA Optical Ground Station – Ten Years Since First Light", ESA bulletin 132, November 2007, pp. 34 – 40.

[7]Roth C., Stadelmann D., Arnold F., Benkeser C. and Huang Q., "High-throughput hardware decoder implementation for optical deep-space communications," *Proceedings of the ESA 6th International Workshop on Tracking, Telemetry and Command Systems for Space Applications*, 2013.

[8]Sans M., Sodnik Z., Zayer I. and Daddato R., "Design of ESA's Optical Ground Station for Participation in LLCD", *Proceedings of the International Conference on Space Optical Systems and Applications,* 2012.

[9]K.-J. Schulz, J. Rush et al., "Optical Link Study Group Final Report," IOAG-15b, June 2012.

[10]Arnold F., Mosberger M., Widmer J. and Gambarara F., "Ground receiver unit for optical communication between LADEE spacecraft and ESA ground station", *SPIE Proceedings*, 2014, Vol. 8971, to be published.

[11]D. Giggenbach, P. Becker, R. Mata-Calvo, C. Fuchs, Z. Sodnik, I. Zayer, „Lunar Optical Communications Link (LOCL): Measurements of Received Power Fluctuations and Wavefront Quality", ICSOS - International Conference on Space Optical Systems and Applications, Kobe, Japan, 2014

[12]D. Giggenbach, "Deriving an estimate for the Fried parameter in mobile optical transmission scenarios," Applied Optics, Vol. 50, No. 2,. Optical Society of America, Jan. 2011, p. 222-226